

Constraints on the genesis of gold mineralization at the Homestake Gold Deposit, Black Hills, South Dakota from rhenium–osmium sulfide geochronology

Ryan M. Morelli · Chris C. Bell · Robert A. Creaser · Antonio Simonetti

Received: 3 August 2009 / Accepted: 12 March 2010 / Published online: 14 April 2010
© Springer-Verlag 2010

Abstract The Homestake gold deposit, located in the Black Hills, South Dakota, USA, is one of the largest known hydrothermal gold deposits globally, with total mining production exceeding 40 Moz Au. Rhenium–osmium geochronology of ore-associated arsenopyrite and pyrrhotite was performed in an effort to delineate the timing of gold mineralization in relation to known tectonothermal events in the northern Black Hills. Arsenopyrite yields a rhenium–osmium (Re–Os) age of $1,736 \pm 8$ Ma (mean squared weighted deviation=1.6), consistent with existing age constraints for gold mineralization, whereas Re–Os pyrrhotite data are highly scattered and do not yield a meaningful mineralization age. This is taken to indicate that the Re–Os arsenopyrite chronometer is robust to at least 400°C , whereas the Re–Os pyrrhotite chronometer is likely

disturbed by temperatures of $300\text{--}350^\circ\text{C}$. The Re–Os arsenopyrite age and initial Os ratio (0.28 ± 0.15) are interpreted to indicate that gold was introduced at ca. 1,730 Ma, coincident with the onset of exhumation of crustal blocks and, possibly, the earliest intrusive phases of Harney Peak granite magmatism. New in situ U–Pb monazite analyses from an aplite dike in the east-central Black Hills indicate that granite magmatism was a protracted event, persisting until at least ca. 1,690 Ma.

Keywords Re–Os · Arsenopyrite · Pyrrhotite · Gold · Homestake · Black Hills · Harney Peak granite

Introduction

Measuring absolute geologic time is critical for understanding geologic processes. Unfortunately, only a small proportion of known minerals can be readily “dated” using conventional techniques, making meaningful absolute age information extremely difficult to extract for some geologic events. Hydrothermal ore deposition is an example of an event that has been historically proven difficult to directly date because of a lack of suitable minerals that crystallize contemporaneously with ore and that are resistant to thermal disturbance. Thus, there is a fundamental inability to temporally link the ore-forming event to tectonic processes occurring synchronously within the host terrane, thereby precluding a comprehensive understanding of deposit formation.

A classic example of this problem can be seen with the Homestake gold deposit, located in the northern Black Hills of South Dakota, USA, which has produced >40 Moz Au during mining from 1876 to 2001 and is one of the largest hydrothermal gold deposits known globally (Goldfarb et al. 2005). Due to being hosted almost exclusively by carbonate–

Editorial handling: B. Lehmann

R. M. Morelli (✉)
Saskatchewan Ministry of Energy and Resources,
200-2101 Scarth Street,
Regina, SK, Canada S4P 2H9
e-mail: Ryan.Morelli@gov.sk.ca

C. C. Bell
School of Earth and Environmental Sciences,
James Cook University,
Douglas,
Townsville, Queensland 4814, Australia

R. A. Creaser
Department of Earth & Atmospheric Sciences,
University of Alberta,
Edmonton, AB, Canada T6G 2R3

A. Simonetti
Department of Civil Engineering and Geological Sciences,
University of Notre Dame,
156 Fitzpatrick Hall,
Notre Dame, IN 46556, USA

silicate–sulfide facies iron formation (so-called stratabound, “Homestake”-style gold), as well as its proximity to Tertiary-aged alkaline intrusions, the origin of this deposit has been debated since its discovery. It was regarded as Tertiary in age by many early researchers (e.g., Hosted and Wright 1923; Noble 1950) due to observable cross-cutting relationships between sulfide-bearing veins and Tertiary-aged dikes at other ore occurrences in the area. However, this relationship is not recognized at the Homestake deposit itself, leading many to conclude that the mineralization was more likely related to the Precambrian host rocks (e.g., Paige 1924; Connolly 1927; Gustafson 1933; Slaughter 1968). The “Precambrian vs. Tertiary” debate was eventually resolved by a Pb isotope study of quartz vein-hosted galena from the host iron formation (Rye et al. 1974) that concluded gold mineralization represented ore remobilized from a 2.5 Ga source and was emplaced around 1,600 Ma.

Recognition of a Precambrian mineralizing event, though critical in advancing understanding of deposit genesis, initiated a new debate among researchers. The strong association of the Homestake mineralization with the iron formation spurred a syngenetic sedimentary exhalative model for the origin of gold, supported by Rye et al. (1974) on the basis of the Pb and S isotopic data (Rye and Rye 1974). This model, which views the gold as being locally remobilized from, but originally syngenetic with, the host rock, was subsequently adopted by others (e.g., Redden and French 1989).

A more widely accepted model is that the deposit is epigenetic and contains gold from an external source and that the association of ore with the iron formation is the result of the latter being a favorable chemical trap for gold from a hydrothermal fluid (e.g., Caddey et al. 1991; Frei et al. 2009). Many proponents of this model would classify Homestake as being a typical “orogenic gold deposit” (Groves et al. 1998; Goldfarb et al. 2005) and recognize both the structural control on mineralization and the introduction of gold-bearing fluids at or after the initiation of peak regional metamorphism, as indicated by mineral assemblages from vein selvages in the deposit (Terry et al. 2003).

Recently, rhenium–osmium (Re–Os) sulfide geochronology has emerged as a viable means of dating ore since the parent element (Re) is chalcophile and partitions from a hydrothermal fluid directly into ore-related sulfide minerals. The Re–Os technique has been applied to a variety of sulfide minerals, including molybdenite (Stein et al. 2001; Selby and Creaser 2001a, b), pyrite (Stein et al. 2000; Morelli et al. 2004), pyrrhotite (Lambert et al. 2000; Frei et al. 1998), and chalcopyrite (Mathur et al. 2000). In particular, arsenopyrite has been recognized as an especially valuable Re–Os chronometer for dating orogenic gold deposits (Arne et al. 2001; Morelli et al. 2005, 2007) due to its widespread occurrence and its typical close genetic relationship to gold in these deposits. In this study, we

performed Re–Os geochronology on gold-related (“shear ore”; Caddey et al. 1991) arsenopyrite, as well as cogenetic pyrrhotite, from one sample from the Homestake deposit in an attempt to pinpoint the timing of gold mineralization. Furthermore, the reasonably well-constrained geological history of the Black Hills allows us to make some general observations regarding the ability of the Re–Os arsenopyrite and pyrrhotite chronometers to withstand isotopic disturbance through younger thermal events.

Regional and deposit geology

The Homestake deposit is situated within the northern Black Hills uplift in central South Dakota, USA (Fig. 1). This uplift resulted from doming of the crust above Laramide-aged intrusions and is exposed at the present erosional level as an inlier of predominantly Precambrian rocks surrounded by Phanerozoic cover. Precambrian rocks

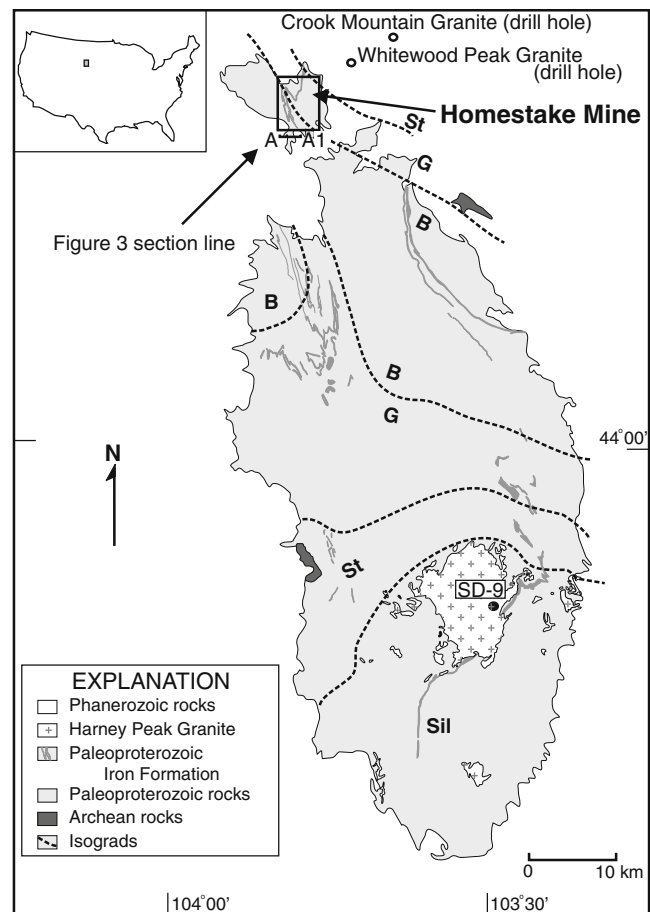


Fig. 1 Geological setting of the Black Hills uplift, South Dakota, USA. Box shows area covered in Fig. 2. B, G, St, and Sil indicate positions of the biotite, garnet, staurolite, and sillimanite isograds, respectively. Modified after DeWitt et al. (1989) and Redden et al. (1990). Sample location for U–Pb monazite dating of Harney Peak granite indicated by “SD-9”

in the uplift record opening of a siliciclastic-dominated basin and its subsequent closure during the collision between the Archean Wyoming and Superior Provinces (Dahl et al. 1999). The regional geology of the Black Hills is thoroughly described by Redden et al. (1990).

Paleoproterozoic rocks of the Black Hills record a progression from a basal assemblage of 2,560–2,480 Ma conglomerate, quartzite, and iron formation (Dahl et al. 2006) into unconformably overlying shallow-water deposits (2,100–1,974 Ma, Redden et al. 1990) that include a range of coarse- to fine-grained clastic sedimentary rocks, iron formation, minor carbonate, and mafic volcanic flows. This sequence was subsequently intruded by metagabbro dikes and/or sills. Deeper water turbiditic and tuffaceous deposits, equivalent in age to shelf quartzites to the north (ca. 1,974 Ma), are present in the central and southern Black Hills, whereas an extensive unconformable sequence of ca. 1,870 Ma conglomerate, turbidites, and basalts is preserved in the east-central portion of the uplift. These Paleoproterozoic sequences suggest deposition in a long-lived intra-continental rift basin (Redden et al. 1990; Houston 1992) or in a backarc basin succeeding earlier rifting (pre-2,170 Ma) of Archean crust (Caddey et al. 1991). Paleoproterozoic and older rocks in the Black Hills uplift were intruded by multiple felsic dikes and sills comprising the ~1,715 Ma “Harney Peak granite” (Redden et al. 1990) exposed in a circular dome in the south-central portion of the uplift (Fig. 1).

The Homestake deposit is exposed in an isolated window on the northern margin of the main Black Hills uplift known as the “Lead window” (Fig. 1). Rocks within this small inlier are equivalent to Paleoproterozoic rocks situated elsewhere in the Black Hills, with the exception of Tertiary intrusions that occur only in the extreme northern portion of the uplift. The Harney Peak granite is not exposed in the Lead window, although granite of approximately equivalent age (1,718±22 Ma, Ghosh et al. 2008) has been intersected by drill hole to the east of the Homestake deposit (Fig. 1; the “Crook Mountain Granite,” Bachman et al. 1990).

The Poorman, Homestake, and Ellison Formations comprise the host sequence of the Homestake deposit (Fig. 2). The Poorman Formation (up to ~1,000 m thick) consists of a lower unit of metatholeiite of oceanic affinity (“Yates Member”; Caddey et al. 1991) overlain by carbonate-bearing pelitic to semipelitic metasediments. The overlying Homestake Formation comprises a thin (0–125 m), metamorphosed, carbonate–silicate–sulfide facies iron formation which hosts almost all gold mineralization at the Homestake deposit. It is dominated locally by Fe carbonate (siderite) or Fe silicate (grunerite) minerals, as well as quartz, biotite, and chlorite. The Homestake Formation is unconformably overlain by the Ellison Formation, a quartzite-dominated unit that marks regional uplift and a

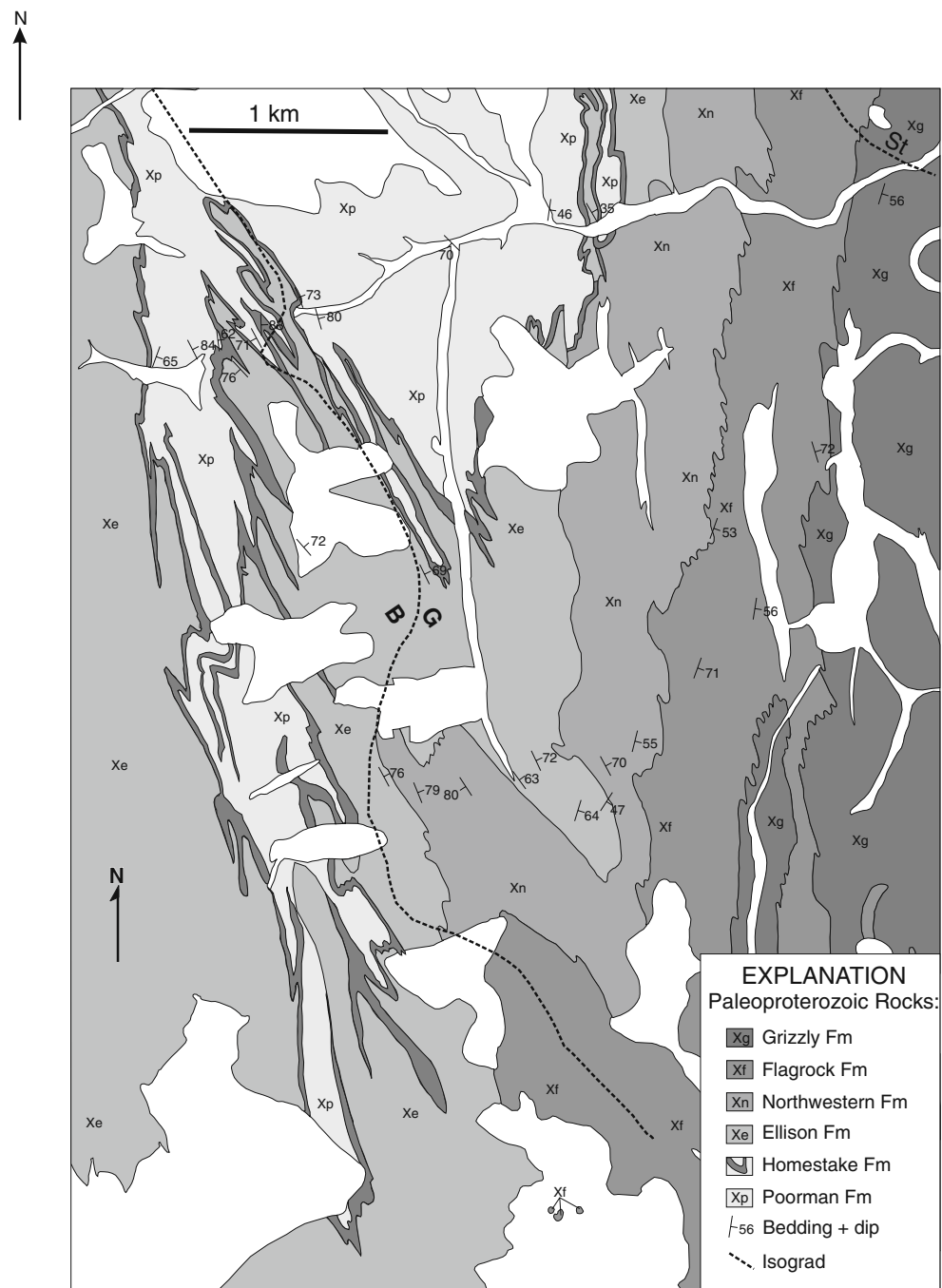
transition from deep-water deposition of turbidites (Poorman Formation) and iron formation (Homestake Formation) into a shallow water environment. Whereas a gabbroic sill believed to be an intrusive equivalent of the Yates Member has been dated at 2,012±3 Ma (Hark et al. 2008), zircons derived from a tuff bed at the base of the Ellison Formation yielded a U–Pb age of 1,974±8 Ma (Redden et al. 1990). Together, these results are interpreted to provide an age bracket of 2,012–1,974 Ma for deposition of the Homestake Iron Formation (Hark et al. 2008).

The structural development of the Homestake Mine is described in several previous studies, as summarized in Table 1. Together with our own observations, five discrete deformation events (D₁ to D₅, oldest to youngest) are identified. The earliest event (D₁) produced a gently dipping, layer-parallel foliation (S₁); locally preserved relicts of S₁ observed in thin section are consistently parallel to bedding. This fabric is probably equivalent to that recognized in the southern Black Hills that was dated at ca. 1,785–1,775 Ma and related to north-directed accretion of the Yavapai island arc (Dahl et al. 2005a, b). The second event (D₂) produced upright, tight to isoclinal F₂ folds that plunge to the SSE (F₂ trends 146°; Fig. 2) with an intense, steeply dipping axial plane foliation (S₂) that forms the dominant cleavage in the area. This event has been attributed to continental collision between the Wyoming and Superior Cratons starting at around 1,760–1,750 Ma (Dahl et al. 1999) and resulted in the development of the N- to NW-trending, upright, isoclinal folds present throughout the Black Hills and peak metamorphic mineral assemblages in the Homestake area. In particular, this collision is responsible for the large-scale geometry of two large anticlinoria (“Lead” and “Poorman” anticlinoria, Fig. 2).

The third recognized deformational phase (D₃) produced a heterogeneously developed sub-horizontal foliation (S₃) which rotates S₂ into a sub-parallel orientation where most prominent. The effect of D₃ has been dramatically obscured by intense folding caused by a subsequent (D₄) event, and the significance of this earlier event has thus gone largely unrecognized. The D₄ event produced tight folds in the Homestake Formation that re-fold F₂ folds about moderate to gently S to SSE plunging axes and that dominate map and cross-sectional patterns. The main stage of gold mineralization at Homestake is interpreted to have been synchronous with this deformational event (Caddy et al. 1991; Table 1). The last recognized phase of deformation (D₅) produced flat lying, millimeter-scale zones of shearing with horizontal axial planes that consistently display a top to the west shear sense. The S₄ fabric initially formed vertically but now dips steeply to the east due to the top to the west rotational effects of D₅.

Gold mineralization in the Homestake deposit is associated with shear zone-hosted quartz veining and is concen-

Fig. 2 Structural and lithological map of Paleoproterozoic rocks from the eastern side of the Lead dome of the Black Hills uplift with bedding measurements. Geology after USGS Quadrangle sheets, Isograds after Caddey et al. (1991)



trated within relatively undeformed ore bodies that exhibit an overall tabular morphology. Mineralization was emplaced into dilated segments of shear zones during a period of “retrogressive hydrothermal alteration” that overprints prograde metamorphic fabrics (Caddey et al. 1991). Whereas ore bodies are strongly concentrated within smaller synclinal structures (equivalent to odd-numbered ore “ledges”; Fig. 3) on the anticlinorium limbs, the adjacent anticlinal structures (even-numbered ore ledges) are nearly devoid of gold mineralization. Gold has a cogenetic relationship with both pyrrhotite and arsenopyrite in the Homestake deposit

(Caddey et al. 1991) and is typically concentrated within alteration zones containing any or all of the minerals chlorite, biotite, sericite, carbonate, and quartz.

Sample selection and analytical procedures

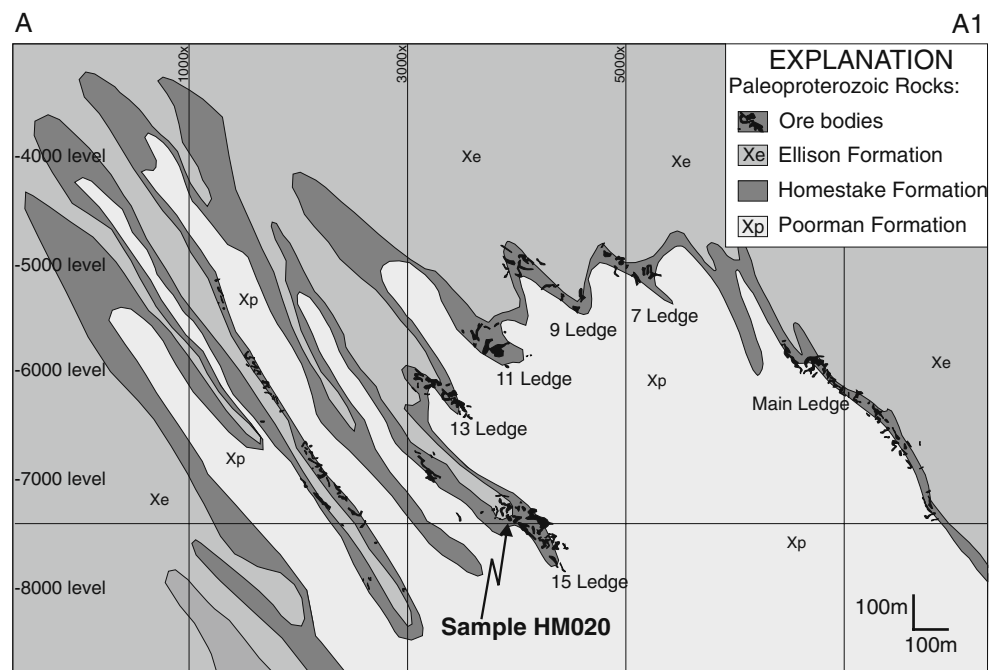
Re–Os sulfide geochronology

Re–Os isotopic analyses were performed on arsenopyrite and pyrrhotite from a sulfide-rich hand specimen (HM020)

Table 1 Summary of deformational events in the Homestake Mine area

This report	Chinn (1969)	Reid (1982)	Meier (1992)	Caddey et al. (1991)
D ₁ —Bedding (S ₀) parallel schistosity (S ₁), locally preserved relicts of S ₁ observed in thin section	D ₁ —Produced a bedding parallel schistosity	D ₁ —Recumbent isoclinal folding of easterly trend, east trending sub-cylindrical ore shoots developed either as original sedimentary accumulation trends or through metamorphic recrystallization of syngenetic metals in sedimentary rocks	D _{1a} —Isoclinal folds with axial planar schistosity	D _{1a} early—Regional plate scale shearing and folding
D ₂ —Large-scale Poorman-Lead anticlinorium fold structure. S ₂ forms the main cleavage in the area, a steep N/NW-striking fabric	D ₁ —Coaxial SE-plunging isoclinal folds	D _{2a} —Overturned isoclinal folds of north westerly trend (Homestake syncline and related folds) D _{2b} —Crossed by steeper conical isoclinal folds on more westerly trends (lower 9 and 11 ledge rotated into D _{2a,b} trends)	D _{1b} —Strongest schistosity trends toward 150° with associated tight to isoclinal folds plunging 24° toward 150° D _{1c} —Large-scale anticlinorium structure plunging 27° toward 120–190°, axial trends of 149–143° and an overturned axial plane dipping 65° toward the SW	D _{1a} early—Regional plate scale shearing and folding
D ₃ —Large-scale D ₃ fold within the mine produced by a shallow fabric, shear sense on S ₂ is top to the east N of the mine and top to the west S of the mine	Noted flat fabric, did not assign relative timing or attribute to any event			D _{1a} middle—Flattening event with no lineation
D ₄ —When D ₄ forms a new fabric it is preserved as a differentiated crenulation cleavage slightly oblique to S ₂ . The S ₄ crenulation cleavage commonly formed by reactivation of S ₂ to produce a composite S ₂₋₄ cleavage	D ₂ —Coaxial crenulation cleavage axial planar to F ₂ folds	D _{2c} —Upright isoclinal folds (more westerly) with parallel ore shoots D _{2d} —Restricted occurrence of open upright, conical isoclinal folds (northwesterly trend)	D _{2b} —Folds axial trace 135–120° and plunge approximately 44° SE with vertical axial plane with open fold forms in restricted 75- to 150-m-wide zones.	D _{1a} late—Sheath folding with axial fabric D _{1b} early—Upright folding with vertical axial plane foliation D _{1b} middle—Ductile brittle shearing accompanied by ore stage mineralization
D ₅ —Small-scale zones of shearing with horizontal axial planes consistently show top to the west shear sense	D ₃ —Differentiated spaced crenulation cleavage (kink fabric) bends F1 and F2 fold axes	D ₃ —North-trending crenulation cleavage and associated F ₃ folds D ₅ —Shallow-dipping north-trending kink fold shears		D _{1b} late—Post ore brittle shearing and crenulation kink fabric

Fig. 3 East–west cross-section looking north through mine 8500N at the Homestake Mine with subsurface geology and the location of sample HM020 from 15 Ledge. See Fig. 1 for section location



from the Homestake underground mine. Specifically, the sample was retrieved from Ore Ledge #15 (Fig. 3), a synclinal structure on the eastern limb of the Poorman anticlinorium. It comprises metamorphosed and hydrothermally altered Homestake iron formation and contains predominantly chlorite (~30–35%), Fe carbonate (~20%), biotite (5–10%), and quartz (<5%) in addition to ore-related pyrrhotite (~20%) and arsenopyrite (15%) and traces of graphite, chalcopyrite, and sphalerite. In detail, arsenopyrite forms large euhedral crystals, ~3 mm to 1 cm in size, dispersed throughout the sample (Fig. 4). Pyrrhotite occurs as coarse (~2–5 mm) anhedral grains or “blebs” that are irregularly distributed within carbonate-rich ovoid bodies and on the margins of coarse arsenopyrite crystals or, alternatively, as granular aggregates (layers) elongated within the trend of the foliation (Fig. 4a). Pyrrhotite layers are intergrown with pyrrhotite blebs. Both pyrrhotite occurrences and the coarse arsenopyrite are cogenetic with gold at Homestake (“shear ore”; Caddey et al. 1991). Although two small individual grains of native gold occur (1) at the margin of, and (2) in a fracture within a large arsenopyrite crystal, most gold in this sample is observed as small (~1–25 μm) angular inclusions within, but near the margins of, the coarse arsenopyrite crystals.

Individual arsenopyrite crystals were isolated from sample HM020 for Re–Os isotopic analysis using an agate pestle and further crushed to a sub-millimeter grain size using an agate mortar and pestle. An attempt was made to select arsenopyrite crystals devoid of pyrrhotite on their margins, and a hand magnet was applied to the crushed fractions to further purify the arsenopyrite. Pure pyrrhotite fractions were obtained by crushing portions of sample

HM020 containing abundant pyrrhotite stringers using an agate shatterbox, followed by sieving (70–100 mesh), methylene iodide density separation, and Frantz magnetic separation. Total sample weights for individual samples



Fig. 4 a Photograph of sample HM020, showing pyrrhotite (*po*) surrounding arsenopyrite (*apy*) crystals and exhibiting parallelism to the foliation (*S*). b Photomicrograph of sample HM020 (field of view = 0.64 mm)

depended on Re content and ranged from ~58 to 170 mg for arsenopyrite and from ~250 to 425 mg for pyrrhotite (Table 2).

The analytical protocol follows that described by Selby and Creaser (2001a, b), with minor modifications. In detail, the crushed sulfide fractions were weighed and added, along with a known amount of mixed ¹⁸⁵Re + ¹⁹⁰Os spike solution and 11 ml of inverse aqua regia (8 ml HNO₃+3 ml HCl) to a borosilicate Carius tube immersed in a methanol + solid carbon dioxide slurry. The top of the tube was then sealed using a natural gas + oxygen torch with the contents still frozen, thereby inhibiting the release from the tube of any OsO₄ from the sample or spike. The sealed tube was allowed to thaw at room temperature and was then placed in a steel jacket and into an oven for ~24 h at 240°C to facilitate complete sample digestion and sample/spike equilibration (i.e., the “Carius tube method”; Shirey and Walker 1995). Upon cooling, the exterior of the tube was cleaned with deionized water and immersed in liquid nitrogen to completely freeze all contained liquids and gases. While frozen, 4 ml of chloroform (CHCl₃) was added, and the contents were then emptied into a polypropylene, 50-ml centrifuge vial and centrifuged for 1–2 min. Osmium partitions strongly into the chloroform, which was then extracted from the aqua regia and placed into a glass vial containing 3 ml of 9 N HBr (solvent

extraction technique described by Cohen and Waters 1996). This extraction was repeated twice more; the glass vial containing CHCl₃, HBr, and the Os fraction was then capped and placed on a 70°C hotplate overnight to reduce Os to the bromide form. The remaining aqua regia, which contains the Re fraction, was dried down in an uncovered glass vial.

Once cooled, the HBr is extracted from the CHCl₃ and dried down on a watch glass covered with Teflon tape. Just prior to complete drying, the droplet is taken up in a thin disposable pipette and placed onto the lid of the glass vial that held the CHCl₃/HBr mixture. The lid is covered with an inverted conical Savillex vial containing 20 µl of 9 N HBr and Os oxidized with a Cr^{VI} + H₂SO₄ mixture (30 µl) on a heating block at 80°C for ~3 h. The droplet was then redried back onto the vial lid, the microdistillation (Birck et al. 1997) was repeated, and the droplet was dried down in the apex of the Savillex conical vial at 60°C and under nitrogen gas.

To recover Re, the aqua regia residue was redissolved in 3 ml of 0.2 N HNO₃, placed in a centrifuge tube, and centrifuged at 5,000 rpm for 5 min. The Re was removed from this solution via anion exchange column chromatography (Morgan et al. 1991) with Eichrom analytical grade anion exchange resin (1×8, 100–200 mesh) in a modified disposable pipette. The eluate was dried down in a PMP

Table 2 Re–Os isotopic data for Homestake arsenopyrite and pyrrhotite

Sample	Sample wt. (g)	¹⁸⁷ Re (ppt)	2σ	¹⁸⁷ Os ^a (ppt)	2σ	¹⁹² Os (ppt)	¹⁸⁷ Re/ ¹⁸⁸ Os	2σ	¹⁸⁷ Os/ ¹⁸⁸ Os	2σ	Error. corr. (ρ)	Model age (Ma) ^a
Arsenopyrite												
H-1a	0.130	39780	140	1168.5	7.8	16.0	7860	280	231.2	8.4	0.978	1740±13
H-2a	0.058	2114	11	62.15	0.87	13.1	513	50	15.3	1.5	0.994	–
H-2b	0.093	7901	29	230.1	3.1	3.11	8100	2100	235	60	0.999	1725±24
H-2c	0.096	15590	57	454.2	5.3	3.99	12400	2400	362	70	0.998	1725±21
H-2d	0.099	2741	11	81.0	1.7	21.3	408	15	12.30	0.50	0.907	–
H-3b	0.107	25344	92	746.0	4.6	10.8	7450	480	220	14	0.994	1743±12
H-3c	0.166	18807	68	545	13	3.56	16700	2100	485	62	0.983	1716±41
Pyrrhotite												
H-P1a	0.423	390.9	1.7	9.84	0.20	15.70	80.40	1.10	2.31	0.03	0.823	–
H-P1(ex)a	0.419	205.9	1.2	5.62	0.10	12.63	52.93	0.83	1.74	0.03	0.886	–
H-P2a	0.412	174.0	1.2	6.41	0.25	25.79	21.63	0.28	1.09	0.02	0.491	–
H-P1b	0.412	326.0	1.6	5.87	1.20	23.19	45.13	0.42	1.10	0.01	0.798	–
H-P2b	0.400	242.9	1.4	10	0.76	15.07	52.17	0.74	2.44	0.03	0.862	–
H-P1c	0.324	321.3	1.7	9.47	0.84	16.59	62.86	0.96	2.14	0.03	0.906	–
H-P2c	0.310	180.2	1.5	5.3	1.20	23.67	24.54	0.33	1.01	0.01	0.732	–
H-P1d	0.246	266.8	2.0	6.08	1.70	32.62	26.32	0.32	0.89	0.01	0.701	–
H-P1(ex)d	0.263	158.3	1.7	4.61	0.50	9.91	53.2	1.7	1.84	0.06	0.926	–
H-P2d	0.255	326.8	2.0	8.88	0.71	14.06	76.4	1.7	2.37	0.05	0.945	–

^a Single mineral model ages assume no initial Os and are calculated only for analyses with ¹⁸⁷Re/¹⁸⁸Os>5,000 (Stein et al. 2000)

beaker at 70°C. The remaining Re-bearing solid was redissolved in 200 µl of 0.05 N HNO₃ and placed into a 1.5-ml polypropylene centrifuge tube, along with a single Dowex AGI-X8 (<20 mesh) anion exchange bead. The bead was agitated in the solution for ~8 h and was then removed and placed into another centrifuge tube containing 1 ml of 6 N HNO₃ for ~8 h. The solution was extracted from the vial and dried down on a hotplate at ~70°C.

In preparation for spectrometry, the purified Os fraction was dissolved in ~0.3 µl of 9 N HBr and deposited onto a crimped Pt filament using a micropipette. The Re fraction was dissolved in ~0.35 µl of 16 N HNO₃ and is transferred from the watch glass onto a Ni wire filament that was previously crimped and glowed at ~2.5 A under atmospheric conditions. Once deposited onto the filament, the Re and Os samples were covered with Ba(NO₃)₂ and Ba(OH)₂/NaOH activator solutions, respectively. Re and Os isotopic compositions were determined by NTIMS (Creaser et al. 1991; Völkening et al. 1991) using a Micromass Sector 54 thermal ionization mass spectrometer at the University of Alberta Radioisotope Facility. All Re isotopic analyses were measured by static Faraday collector analysis, whereas Os isotopic abundances were measured by an ETP electron multiplier in pulse counting mode. Error propagation included consideration of all relevant sources of analytical error, including uncertainty in Re and Os blank levels and Os blank isotopic composition, monitored variations in Re and Os standards, and ¹⁸O/¹⁶O ratios of the measured Re and Os oxides. To account for the highly correlated uncertainties typical of highly radiogenic sulfide samples (Stein et al. 2000), an error correlation factor was applied (Schmitz and Schoene 2006, Eq. 71) that assesses the degree of correlation between uncertainties in the ¹⁸⁷Re/¹⁸⁸Os and ¹⁸⁷Os/¹⁸⁸Os ratios for a given analysis. Total procedural blanks (*n*=7) varied slightly depending on the batch and volume of HNO₃ used (arsenopyrite: Re=1.2 pg, Os=0.3 pg, ¹⁸⁷Os/¹⁸⁸Os [Os_{IC}]=0.27; pyrrhotite: Re=1.6 pg, Os=0.09 pg, Os_{IC}=0.23). At these levels, blank contribution accounts for <0.6% (Re) and <0.3% (¹⁸⁷Os) for arsenopyrite analyses and <2.4% (Re) and <0.21% (¹⁸⁷Os) for pyrrhotite analyses. Isochron regression was performed using Isoplot v3.00 (Ludwig 2003) using the ¹⁸⁷Re decay constant of Smoliar et al. (1996).

U–Pb monazite geochronology

To further constrain the timing of intrusion of the Harney Peak Granite, specifically in relation to gold mineralization, five hand samples were collected from outcrop of both the Calamity Peak satellite intrusion and the main mass of the Harney Peak granite. Polished petrographic thin sections were made of these samples, which were then scanned for Th by X-ray mapping using an electron microprobe to

facilitate monazite identification. Only two of the five samples (SD-9A, -9B) contained monazite in sufficient quantity and of sufficient size to be useful for in situ thin-section analysis. A single zircon crystal was also identified, but was strongly metamict and too small for isotopic analysis. Both samples were from an aplitic dike (1- to 2-mm grain size) situated in the main exposure of the Harney Peak pluton (Fig. 1) and consist primarily of equigranular K-feldspar, quartz, muscovite, and biotite.

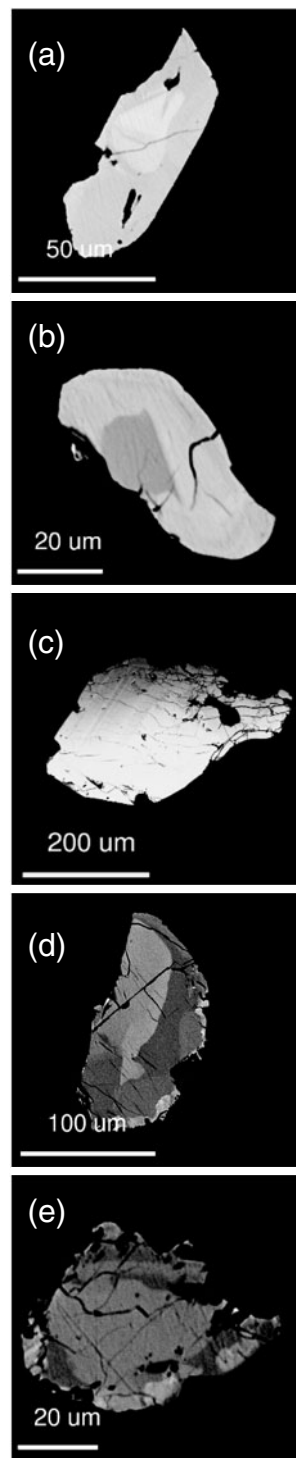
Five individual monazite crystals, ranging in diameter from ~20 to 250 µm (Fig. 5a–e), were used from the Harney Peak granite samples SD-9A and -9B for U–Pb geochronology. U–Pb isotopic analyses were performed by the in situ petrographic thin-section technique described by Simonetti et al. (2006) using a New Wave Research UP213 laser ablation system coupled to a *Nu Plasma* multi-collector ICP-MS. Individual spot sizes for ablation analyses were 12 µm; all other instrument parameters and measurement protocol are identical to those described by Simonetti et al. (2006). Analysis of an external standard from the Eleys Creek region of western Australia (Simonetti et al. 2006) was performed using a 12-µm spot size both prior to and following all sample analyses, and a 30-s blank measurement was performed prior to laser ablation.

Results

Rhenium–osmium

Seven analyses of arsenopyrite and ten of pyrrhotite from sample HM020 were performed, and the results are reported in Table 2. These data reveal a strong contrast in Re contents between the two minerals from this sample. Arsenopyrite shows relatively high but variable Re content (~3.5–63 ppb), whereas pyrrhotite Re contents are much lower and more consistent (~0.3–0.6 ppb). Common Os contents for both minerals were comparable, as indicated by ¹⁹²Os concentrations (arsenopyrite = 0.003–0.021 ppb; pyrrhotite = 0.009–0.032 ppb; Table 2). The variation in total Re (and corresponding radiogenic ¹⁸⁷Os) and common Os contents between arsenopyrite and pyrrhotite resulted in a large range in ¹⁸⁷Re/¹⁸⁸Os and ¹⁸⁷Os/¹⁸⁸Os ratios. On a conventional ¹⁸⁷Re/¹⁸⁸Os vs. ¹⁸⁷Os/¹⁸⁸Os plot, regression of all seven arsenopyrite analyses results in a Model 1 isochron with an age of 1,736±8 Ma (2σ; mean squared weighted deviation (MSWD)=1.6, initial ¹⁸⁷Os/¹⁸⁸Os ratio [Os_i]=0.28±0.15; Fig. 6a). The high precision of the age is a function of the large spread between data points (¹⁸⁷Re/¹⁸⁸Os=~400–17,000) and the excellent fit of data to the regression line. The decreased precision in the determined Os_i is due to the lack of data that plot near the y-axis. Five of the seven Homestake arsenopyrites qualify

Fig. 5 Electron microprobe photomicrographs of monazite crystals from thin sections of Harney Peak granite used for in situ laser ablation U–Pb geochronology. Samples are 9A-1 (a), 9A-3 (b), 9B-1 (c), 9B-3 (d), and 9B-4 (e)



as “low-level highly radiogenic” samples (i.e., $^{187}\text{Re}/^{188}\text{Os} > 5,000$; Stein et al. 2000) and can be used to calculate single mineral model ages, assuming no initial Os (Stein et al. 2000). Model ages for these five samples range from ca. 1,743 to 1,716 Ma (Table 2), identical (within associated 2σ uncertainties) to the Re–Os arsenopyrite isochron age. Regression of the five most radiogenic arsenopyrite analyses in ^{187}Re vs. ^{187}Os space (Stein et al. 2000) also

yields an identical result ($1,744 \pm 14$ Ma, 2σ , $\text{MSWD} = 0.74$; not shown).

In contrast to the arsenopyrite, pyrrhotite analyses are highly scattered on a $^{187}\text{Re}/^{188}\text{Os}$ vs. $^{187}\text{Os}/^{188}\text{Os}$ plot (Fig. 6b). Owing to the consistency of Re and common Os concentrations, the spread between pyrrhotite data points is much more restricted than for arsenopyrite, with a range in $^{187}\text{Re}/^{188}\text{Os}$ from ~20 to 80. The collective regression of all ten pyrrhotite analyses yield a Model 3 errorchron “age” of $1,558 \pm 680$ Ma ($\text{MSWD} = 2674$, $\text{Os}_i = 0.4 \pm 0.6$ Ma). Only three of the pyrrhotite analyses plot on the arsenopyrite regression line, whereas the seven remaining pyrrhotite data scatter both above and below the arsenopyrite isochron. The lack of observable textural differences between the pyrrhotite which used these for three analyses and those that show scattered Re–Os isotopic systematics obscures the significance of the variable pyrrhotite results.

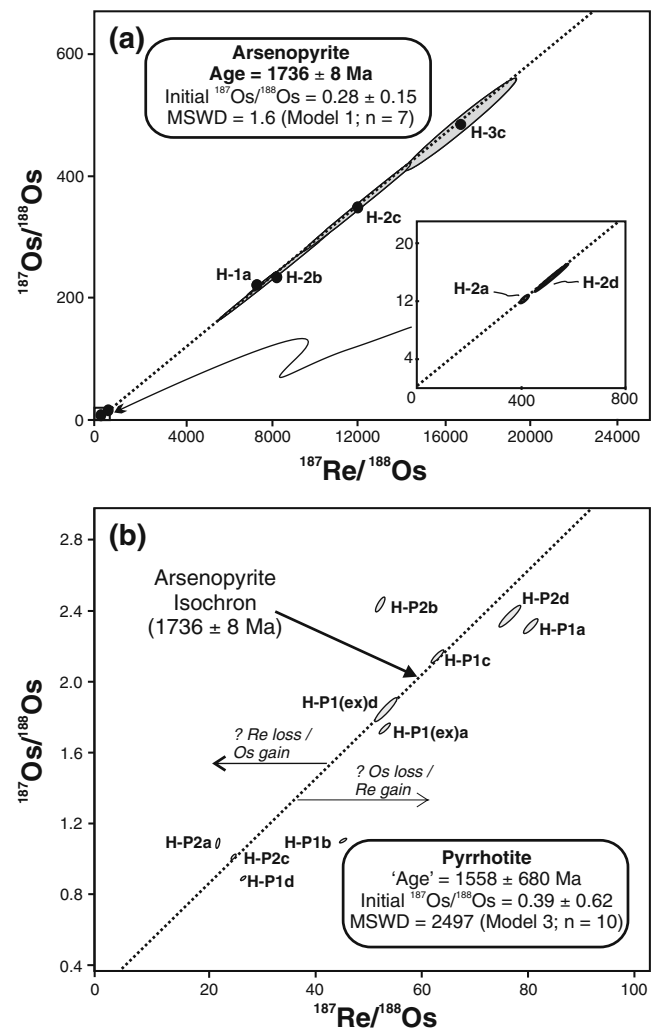


Fig. 6 **a** Conventional Re–Os isochron plot based upon analyses of arsenopyrite from the Homestake deposit. **b** Results of linear regression of Re–Os analyses of Homestake deposit pyrrhotite, with reference to the Re–Os arsenopyrite isochron from (a)

Uranium–lead

In total, 27 U–Pb isotopic analyses were performed using laser ablation mass spectrometry on two monazite crystals from thin section 9A and on three monazite crystals from thin section 9B (Table 3). All monazites analyzed have relatively high U, Th, and Pb concentrations, and only four of the 27 analyses yielded detectable common Pb. Though detectable, ^{204}Pb contents in these four analyses were low and were corrected for prior to age calculation.

All monazite analyses are concordant within associated 2σ uncertainties. Inspection of $^{207}\text{Pb}/^{206}\text{Pb}$ ages from spatial groupings of each of the crystals reveals two distinct age populations. Nineteen analyses of samples 9A and 9B yield a weighted mean $^{207}\text{Pb}/^{206}\text{Pb}$ age of $1,694.2\pm 2.4$ Ma (2σ ; MSWD=0.75, probability = 0.76; Fig. 7a). The remaining eight analyses, which include all analyses of sample 9B-3 except for 9B-3-6, yield apparent $^{207}\text{Pb}/^{206}\text{Pb}$ ages between 1,675 and 1,686 Ma and a weighted mean $^{207}\text{Pb}/^{206}\text{Pb}$ age of $1,682.5\pm 3.4$ Ma (2σ ; MSWD=0.62, probability = 0.74; Fig. 7a). Analysis 9B-3-6, from the central region of monazite grain 9B-3 (Fig. 5d), yields an apparent $^{207}\text{Pb}/^{206}\text{Pb}$ age of $1,699\pm 11$ Ma and is included within the first regression. However, a different interpretation of these data is also possible. When plotted on a cumulative probability plot, the determined $^{207}\text{Pb}/^{206}\text{Pb}$ ages from all analyses resemble a normal distribution (Fig. 7b; 26 of 27 analyses) and define a weighted mean $^{207}\text{Pb}/^{206}\text{Pb}$ age of $1,691.0\pm 2.6$ (2σ ; MSWD=1.6; 26 of 27 analyses). The possible significance of each of these age interpretations is discussed further in the next section.

Discussion

Significance of Re–Os results

Assessing the significance of the Re–Os arsenopyrite and pyrrhotite data with respect to the timing of gold mineralization is best achieved by comparison to existing age constraints for this event. Prior to this study, the sole reported age determination directly on ore-related minerals at Homestake was from a combination of bulk Pb and Pb stepwise leach (PbSL) data from arsenopyrite (Frei et al. 2009), which defined an isochron yielding an age of $1,715\pm 66$ Ma ($1,719_{-45}^{+38}$ Ma, 2σ , by robust regression). Ghosh et al. (2008) have also interpreted a $1,718\pm 22$ Ma upper-intercept magmatic age (2σ) from 16 of 32 U–Pb analyses of extensively metamict (high U) zircons from the Crook Mountain pegmatite, situated in the vicinity of the deposit (Fig. 1), to date the gold mineralizing event on the basis of an inferred genetic relationship between the two events.

There exists widespread agreement that the Homestake mineralizing event postdated peak regional metamorphism (D_2/S_2 ; Table 1) due to overprinting of peak metamorphic mineral assemblages by hydrothermal alteration assemblages related to gold emplacement (Caddey et al. 1991; Frei et al. 2009). The timing of S_2 axial planar cleavage development has been dated at $1,746\pm 10$ Ma from PbSL of allanite and/or monazite inclusions in Homestake Formation-hosted garnet (Frei et al. 2009; Fig. 8). This determination is consistent with other independent dates for this event in the Black Hills, including a $^{40}\text{Ar}/^{39}\text{Ar}$ hornblende age of $1,742\pm 10$ Ma (Dahl et al. 1999) and a total Pb monazite age of $1,750\pm 10$ Ma (Dahl et al. 2005a, b). Peak metamorphic conditions might have persisted until the commencement of regional unroofing, believed to have occurred at $1,732\pm 9$ Ma, (Dahl et al. 2005b); this date could thus provide a maximum age bracket for gold mineralization (Frei et al. 2009). The minimum age bracket for gold mineralization is considered by Frei et al. (2009) to be $1,713\pm 10$ Ma based on their PbSL isochron date for monazite from the “Whitewood Peak pegmatite” (Fig. 1), which they consider to be contemporaneous with post-ore shearing of the Homestake deposit (following Caddey et al. 1991).

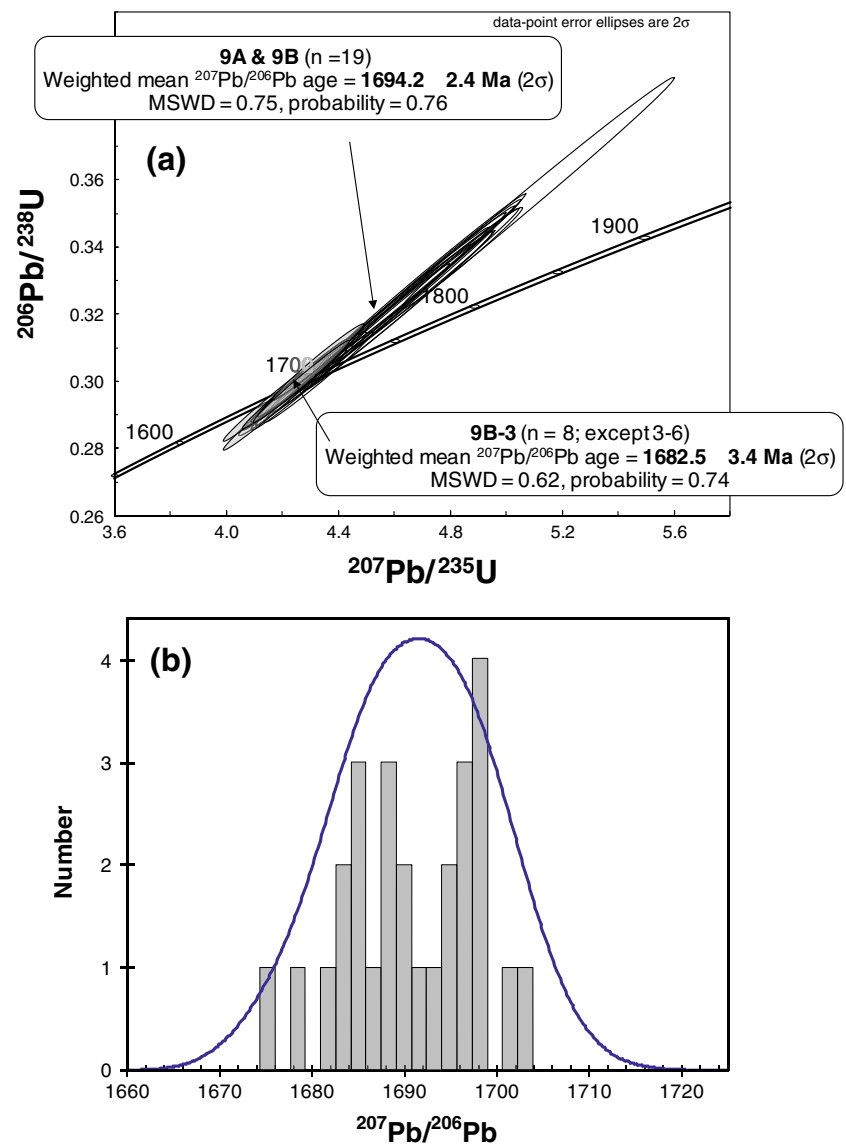
In addition to being highly imprecise, it is clear from the high degree of scatter that the Re–Os isotopic compositions in Homestake pyrrhotite have been disturbed and do not yield meaningful information about the timing of ore emplacement. In contrast, the relatively precise Re–Os arsenopyrite age of $1,736\pm 8$ Ma is in good agreement with the proposed age bracket of Frei et al. (2009) of $1,732\pm 9$ to $1,713\pm 10$ Ma for main stage gold mineralization at Homestake (Fig. 8). It is also consistent, within associated uncertainties, with their Pb–Pb arsenopyrite isochron age and the inferred mineralization age of Ghosh et al. (2008). For these reasons, and because of the close paragenetic relationship between arsenopyrite and gold in the deposit (Caddey et al. 1991), we consider the Re–Os arsenopyrite age to represent the time at which main stage gold mineralization took place at the Homestake deposit.

An interesting characteristic of the Re–Os isotopic compositions of Homestake arsenopyrite is the significant spread of data along the isochron (i.e., $^{187}\text{Re}/^{188}\text{Os}$ ratios ranging from 408 to 16,700; Table 2). The significance and cause of this variation is currently unclear. Frei et al. (2009) speculated that inclusions of allanite and/or monazite were the cause of relatively high $^{208}\text{Pb}/^{206}\text{Pb}$ compositions (relative to an arsenopyrite and common lead mixing line) measured for some “shear ore” arsenopyrite they analyzed. They interpreted these radiogenic phases to cause skewing of results toward older ages such that the resulting $1,719_{-45}^{+38}$ Ma robust regression date should be viewed most appropriately as a maximum age for arsenopyrite crystallization. The

Table 3 U–Pb isotopic data for Harney Peak granite monazite

Grain/analysis no.	²⁰⁴ Pb cps	²⁰⁶ Pb cps	²⁰⁷ Pb/ ²⁰⁶ Pb	²⁰⁷ Pb/ ²³⁵ U	²⁰⁶ Pb/ ²³⁸ U	ρ	²⁰⁷ Pb/ ²⁰⁶ Pb apparent age (Ma)	²⁰⁶ Pb/ ²³⁸ U apparent age (Ma)	$\pm 2\sigma$	$\pm 2\sigma$	% discord.
9A-1											
-1	0	1,846,188	0.10410	4.714	0.273	0.0190	1,698	1,831	± 11	± 106	-8
-2	60	489,646	0.10406	4.841	0.179	0.0124	1,698	1,870	± 11	± 69	-10
9A-3											
-1	0	813,090	0.10433	4.331	0.158	0.0110	1,703	1,697	± 10	± 62	0
-2	100	1,260,174	0.10423	4.329	0.142	0.0098	1,701	1,706	± 13	± 55	0
-3	0	1,514,240	0.10389	4.258	0.140	0.0098	1,695	1,679	± 11	± 55	1
9B-1											
-1	0	1,665,346	0.10393	4.451	0.283	0.0198	1,695	1,745	± 9	± 111	-3
-2	0	1,246,611	0.10400	4.606	0.295	0.0206	1,697	1,798	± 10	± 115	-6
-3	0	2,788,506	0.10356	4.620	0.310	0.0217	1,689	1,807	± 10	± 121	-7
-4	1,000	2,370,122	0.10395	4.615	0.275	0.0191	1,696	1,795	± 12	± 107	-6
-5	0	1,740,174	0.10370	4.679	0.287	0.0201	1,691	1,826	± 10	± 112	-8
-6	0	1,692,077	0.10411	4.617	0.281	0.0195	1,699	1,795	± 11	± 109	-6
-7	0	2,742,664	0.10367	4.594	0.282	0.0198	1,691	1,798	± 10	± 111	-6
-8	0	1,987,878	0.10350	4.738	0.259	0.0182	1,688	1,848	± 10	± 101	-10
-9	0	1,755,524	0.10384	4.569	0.250	0.0174	1,694	1,787	± 10	± 98	-5
-10	0	2,793,019	0.10347	4.701	0.302	0.0212	1,687	1,837	± 10	± 118	-9
9B-3											
-1	0	1,670,799	0.10329	4.141	0.135	0.0095	1,684	1,640	± 9	± 54	3
-2	0	1,231,602	0.10336	4.236	0.131	0.0091	1,685	1,679	± 10	± 52	0
-3	0	1,549,173	0.10281	4.140	0.134	0.0095	1,675	1,653	± 9	± 54	1
-4	0	3,052,690	0.10339	4.237	0.130	0.0091	1,686	1,679	± 10	± 51	0
-5	0	3,479,083	0.10319	4.203	0.128	0.0090	1,682	1,669	± 10	± 51	1
-6	0	1,587,555	0.10412	4.291	0.139	0.0098	1,699	1,699	± 11	± 55	0
-7	0	3,844,246	0.10325	4.265	0.136	0.0095	1,683	1,691	± 10	± 54	0
-8	0	1,711,706	0.10296	4.319	0.134	0.0095	1,678	1,714	± 10	± 53	-2
-9	0	2,742,459	0.10337	4.257	0.142	0.0100	1,686	1,685	± 10	± 56	0
9B-4											
-1	150	994,405	0.10398	5.024	0.471	0.0328	1,696	1,936	± 15	± 181	-14
-2	0	1,093,466	0.10357	4.217	0.132	0.0092	1,689	1,675	± 11	± 52	1
-3	0	1,416,950	0.10367	4.203	0.129	0.0090	1,691	1,665	± 11	± 51	2

Fig. 7 U–Pb isotopic data from laser ablation analyses of monazite from the Harney Peak granite: **a** U–Pb concordia plot, indicating two age domains at 1,694 and 1,683 Ma. **b** Cumulative distribution plot of determined $^{207}\text{Pb}/^{206}\text{Pb}$ ages, which approach a normal distribution centered on a weighted mean $^{207}\text{Pb}/^{206}\text{Pb}$ age of $1,691.0 \pm 2.6$ Ma



possibility that a similar phenomenon is affecting the Re–Os isotopic compositions of arsenopyrite and causing the observed compositional variability cannot be ruled out, but we consider it unlikely for several reasons. First, petrographic examination of arsenopyrite crystals in the specimen revealed no detectable allanite or monazite inclusions. Second, even if older inclusions of these minerals were present, the siderophile–chalcophile geochemical affinity of Re and Os make it unlikely that either allanite or monazite would contain these elements in sufficient concentrations to have a significant effect on the measured isotopic compositions. Third, if older Re- and/or Os-bearing inclusions were present, it would probably be in varying proportions, making it unlikely that the isochronous behavior observed for Homestake arsenopyrite would be preserved. The analyzed Homestake arsenopyrites have ranges in Re–Os concentrations and isotopic compositions that are generally similar to

that observed in other orogenic-style gold deposits around the world (e.g., Arne et al. 2001; Morelli et al. 2005, 2007). From the data (Table 2), it seems evident that for low (Re) level sulfide minerals such as arsenopyrite, even small variations in Re and/or common Os contents between samples can cause significant spread in $^{187}\text{Re}/^{188}\text{Os}$ ratios. Based on available evidence, we maintain the view that these compositions are inherent to the arsenopyrite and do not reflect the presence of radiogenic inclusions.

Timing of granite magmatism and its relation to gold mineralization

The close spatial and temporal association between late orogenic granitoid intrusions and emplacement of orogenic gold deposits globally is well documented (Groves et al. 1998; Goldfarb et al. 2001), although it remains unclear

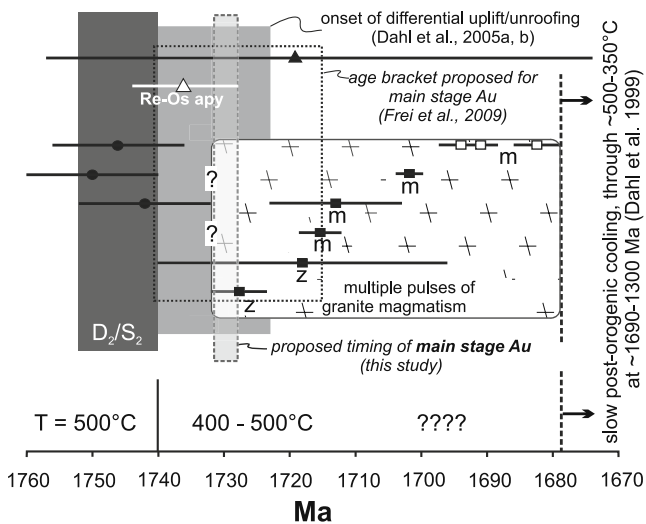


Fig. 8 Compilation of existing geochronologic data that constrain the timing of Homestake gold mineralization. *Unfilled symbols* represent data from the present study. Sources of data not indicated in figure are as follows: for D_2/S_2 development: Dahl et al. (1999, 2005a, b and Frei et al. (2009); for Harney Peak granite magmatism: Redden et al. (1990), Krogstad and Walker (1994), Ghosh et al. (2008), and Frei et al. (2009). Temperature estimates for peak metamorphism in the Homestake area are from Chinn (1969); Kath and Redden (1990); and Caddey et al. (1991) and for syn-gold are from Sharp et al. (1985)

whether there is also a genetic link. This is similar to the case for the Homestake gold deposit where Harney Peak-type granite magmatism is known to exist proximal to the deposit. Structural relationships at the deposit led Caddey et al. (1991) to conclude that gold mineralization must have been concurrent with the early stages of granite emplacement, whereby gold-bearing fluids generated deep within the crust were mobilized during magmatism into shear zones. Frei et al. (2009) also propose a link between granite emplacement and gold mineralization on geochronological grounds and because of overlap between Pb-isotopic compositions of Homestake galena and pegmatitic granite-derived feldspars. This relationship is complicated, however, by the interpretation that later stages of granite emplacement apparently postdate main stage ore (Caddey et al. 1991; Frei et al. 2009). Certainly, knowledge of the full temporal range of granite magmatism in the Black Hills is an important, albeit inadequately understood, benchmark for establishing the timing of ore mineralization.

In performing in situ U–Pb monazite geochronology on a sample of Harney Peak granite, our objective was to temporally constrain the timing of the early stages of Harney Peak magmatism; however, the aplitic dike was the only sample to yield monazite, and the results clearly indicate that this was one of the latest intrusive phases. Nevertheless, these results provide important information on the duration of magmatism in the Black Hills. As

discussed earlier, analyses of multiple monazite grains in the aplite yielded either (1) two, apparently distinct, age populations of 1,694 and 1,683 Ma or (2) a single age of 1,691 Ma, depending on the method of data analysis. The petrogenetic significance of these age determinations can best be determined through an examination of the compositional characteristics of the analyzed grains. Ten of the 19 spot analyses that define the apparent 1,694 Ma age are derived from the >200- μ m diameter 9B-1 grain. Inspection of the back-scattered electron image reveals a clear pattern of concentric zoning in the top left portion of the grain (Fig. 9). This concentric zoning is characteristic of monazite of igneous origin, likely reflecting an evolution in both the magma composition and the equilibrium composition of the monazite as it crystallized (Williams et al. 2007). Whether an age of 1,694 or 1,691 Ma age is accepted for this crystal, the observed zoning confirms that this represents the timing of crystallization of the aplitic phase of the Harney Peak granite.

The validity and possible interpretation of the apparent 1,683 Ma age is difficult to assess but can be further explored using compositional variations within monazite 9B-3. This result is derived from eight of nine analyses of grain 9B-3, with the exception being a single spot analysis (9B-3-6) from the central region of the crystal that yields an apparent $^{207}\text{Pb}/^{206}\text{Pb}$ age of 1,699 Ma (Fig. 10a). A possible explanation for the anomalous age variation in monazite crystal 9B-3 is that this crystal comprises a core that formed during magma crystallization at ca. 1,694 Ma and a younger rim that represents renewed monazite growth around the core at ca. 1,683 Ma (Fig. 10b). To test this hypothesis, yttrium compositional mapping was performed by microprobe to reveal compositional zoning in the crystal

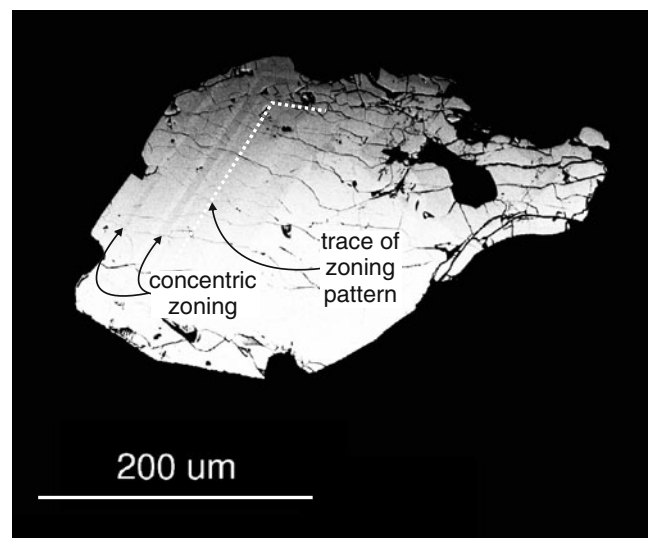
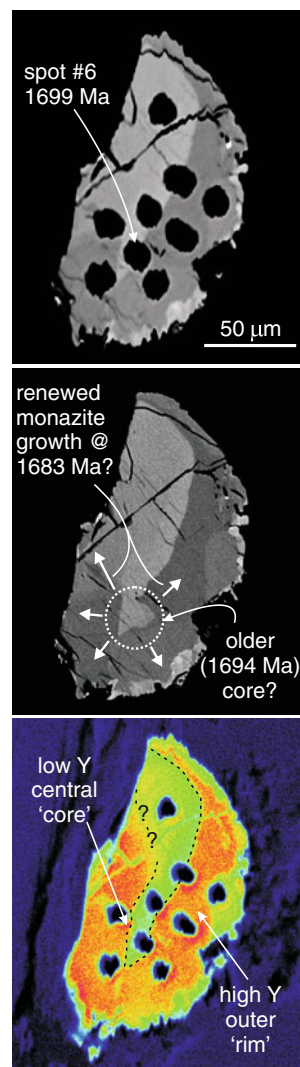


Fig. 9 Electron microprobe photomicrograph showing magmatic zoning in monazite crystal from sample 9B-1 of Harney Peak granite

(e.g., Dahl et al. 2005a, b; Williams et al. 2007). The resulting yttrium distribution map of this grain does confirm the presence of intracrystal chemical zonation, showing a central region with a relatively low yttrium concentration surrounded by a high Y outer region (Fig. 10c). However, this low Y region encompasses an area beyond that of analysis 9B-3-6 and includes an area covered by spot analyses that yielded the apparently younger (1,683 Ma) age. The existing monazite data are thus insufficient to conclusively determine whether monazite growth in this phase of the granite occurred only at 1,691 Ma or over a prolonged period from at least 1,694 to 1,683 Ma.

Previous determinations for the age of granite emplacement in the Black Hills (see summary in Dahl and Foland 2008) and the compositions of granite-hosted fluid inclusions (Sirbescu and Nabelek 2003) are suggestive of a protracted magmatic event, the full temporal range of which might still be unresolved. Although highly discordant, the earliest reported age of $1,727.7 \pm 4.3$ Ma is from the upper

Fig. 10 Electron microprobe photomicrographs of Harney Peak monazite sample 9B-3, showing location of laser ablation pits (a), interpretation of grain history based on U–Pb results (b), and yttrium map of grain in relation to pit location (c). Analyses were performed on polished thin sections using a JEOL JXA-8900R electron microprobe at the University of Alberta. Compositional (yttrium) mapping was done by scanning a focused beam using an accelerating potential voltage of 20.0 kV, a probe current of 1.016 e^{-7} A, and a counting time of 50 ms



intercept of a chord defined by two analyses of metamict zircon obtained from a slightly foliated granite sample (Redden et al. 1990). Despite the discordance, the lower intercept age of 55.3 ± 1.7 Ma is consistent with the occurrence of Pb loss during Tertiary magmatism and/or hydrothermal fluid flow during Laramide uplift. A monazite fraction from this same sample was near concordant and yielded a $^{207}\text{Pb}/^{206}\text{Pb}$ age of 1715 ± 3.2 MA (lower intercept age = 60 ± 20 Ma). It is possible that the discrepancy between the zircon and monazite ages from this single sample arise from the zircons being a xenocrystic phase representative of an early intrusive episode of Harney Peak granitic magmatism. As discussed earlier, discordant zircon from the Crook Mountain Granite in the northern Black Hills has yielded an upper intercept age of $1,718 \pm 22$ Ma (Ghosh et al. 2008), whereas an age of $1,713 \pm 10$ Ma was resolved from monazite inclusions in garnet from a pegmatite intersected in drill core to the northeast of the Homestake deposit (Frei et al. 2009). The youngest recognized granitic magmatism prior to this study is the Tin Mountain Pegmatite in the southern Black Hills based on a $1,702 \pm 2.5$ Ma date from U–Pb analysis of apatite (Krogstad and Walker 1994). Cumulatively, the existing published data for the timing of Harney Peak magmatism could extend from as early as ca. 1,730 Ma to as late as 1,690 or even 1,683 Ma (this study; Fig. 8). Thus, in comparison to the new Re–Os arsenopyrite age presented here, it is possible that the earliest phase of granitic magmatism could overlap with the timing of gold-related sulfide mineralization.

Based on a combination of field relationships, existing geochronological constraints for granitic intrusion, and our new Re–Os age for gold-related arsenopyrite, we propose that the Homestake gold mineralizing event occurred at ca. 1,730 Ma (Fig. 8). Perhaps significantly, this timing also coincides with that proposed for the onset of differential uplift and unroofing of crustal blocks in the Black Hills ($1,732 \pm 9$ Ma; Dahl et al. 2005a, b), the timing of shearing in Homestake Mine (as suggested by Frei et al. 2009), and, possibly, the earliest phase of Harney Peak magmatism.

Significance of initial $^{187}\text{Os}/^{188}\text{Os}$ ratios for gold metallogeny in the Black Hills

As reviewed by Paterson and Lisenbee (1990), various epigenetic models have been proposed for the origin of the Homestake deposit. These include a (remobilized) syngenetic exhalative model (Rye and Rye 1974; Redden and French 1989), an intrusion-related epigenetic model (Caddey et al. 1991; Frei et al. 2009), and a metamorphic dehydration model (Kath 1990; Paterson and Lisenbee 1990). Even within individual models, there is further debate as to the ultimate source of the gold. The

geochronological data presented here add to a framework of information that will help to clarify temporal relationships between Homestake gold mineralization and tectonic events that may have played a role in its origin. However, timing constraints alone do not distinguish between rock types/reservoirs that might have contributed gold to the ore system. In this regard, initial $^{187}\text{Os}/^{188}\text{Os}$ ratios (Os_i) of the Homestake sulfides can provide unique insight into the ore-forming process (e.g., Arne et al. 2001; Morelli et al. 2005, 2007) and can be used to test of the feasibility of individual models. For further perspective on the significance of the arsenopyrite Os_i , a selection of six whole rock samples from the host stratigraphy in the vicinity of the Homestake deposit, perhaps representative of rocks that might have contributed gold (and Os) to the hydrothermal system, were collected for Re–Os isotopic analysis (Table 4). A comparison between the Os isotopic evolution of these samples (Lower Poorman Fm. [Yates Member] amphibolite, Upper Poorman Formation phyllite, Homestake Formation iron formation, and Ellison Formation quartzite) and the Homestake arsenopyrite, from the determined time of deposition/crystallization to the present, is shown in Fig. 11. In making this comparison, however, it must be noted that there is an assumption that the arsenopyrite Os_i is a valid proxy for that of gold and that the Re–Os isotopic composition of the

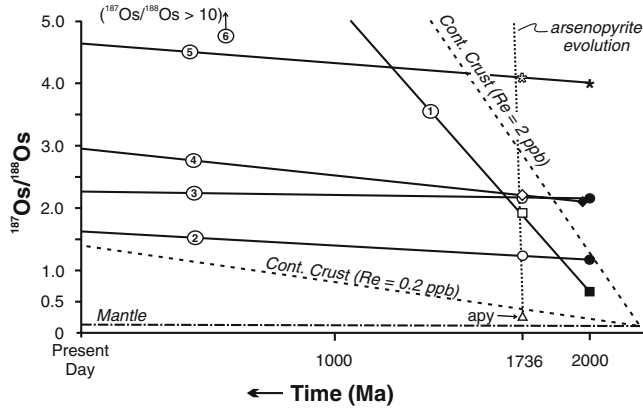


Fig. 11 Osmium isotopic evolution of arsenopyrite (“apy”, open triangle) and samples from units comprising the Homestake deposit host stratigraphy, assuming no post-1,736 Ma change in Re–Os isotopic compositions. Sample labels are: 1 Yates unit amphibolites; 2, 3 Homestake iron formation; 4 Ellison Fm. quartzite; and 5 Upper Poorman Formation phyllite. A second sample of Upper Poorman Formation phyllite (6), characterized by $^{187}\text{Os}/^{188}\text{Os}$ of ~10–10.5 between 2,000 Ma and the present, plots off the scale of the diagram. Closed symbols represent the Os_i of the sample at the time of deposition; open symbols represent the $^{187}\text{Os}/^{188}\text{Os}$ of the sample at the inferred time of gold mineralization (1,736 Ma). Also shown are the isotopic evolution curve of primitive mantle (dashed/dotted line; Meisel et al. 2001) and two models for the Os isotopic evolution of continental crust, assuming extraction from the mantle at 2,200 Ma and lower- and upper-limit total Re concentration of 0.2 ppb (Peucker-Ehrenbrink and Jahn 2001) and 2 ppb (Sun et al. 2003), respectively

Table 4 Re–Os isotopic data for whole rock samples of Homestake deposit host stratigraphic units

Sample	Unit/lithology	Assumed time of deposition (Ma)	Sample wt (g)	Re (ppb)	$^{187}\text{Os}^*$ (^{192}Os ppt)	$^{187}\text{Re}/^{188}\text{Os} \pm 2\sigma$ abs	$^{187}\text{Os}/^{188}\text{Os} \pm 2\sigma$ abs	Os_{IC}^a , present	Os_{IC}^a , 1,736 Ma	Os_{IC} at time of deposition			
1	Yates Member, amphibolite	2,012	1	0.350	306.4	100.20	269	4.73	9.84	0.178	9.84	1.94	0.66
2	Homestake Fm, carbonate-silicate facies iron formation	2,000	0.99	0.085	24.72	53.11	13.3	0.318	1.64	0.022	1.64	1.25	1.19
3	Homestake Fm, carbonate-silicate facies iron formation	2,000	1.02	0.067	3.62	5.30	3.18	0.093	2.27	0.012	2.27	2.18	2.17
4	Ellison Fm, quartzite	1,974	1	0.416	53.94	44.50	25.0	1.08	2.96	0.077	2.96	2.22	2.12
5	Upper Poorman Fm, phyllite	2,012	1.01	1.074	22.67	7.90	18.6	0.144	4.64	0.019	4.64	4.09	4.00
6	Upper Poorman Fm, phyllite	2,012	0.01	18.49	733.2	2775	6.96	0.058	10.5	0.038	10.5	10.3	10.2

^a Os_{IC} Os isotopic compositions; $^{187}\text{Os}/^{188}\text{Os}$ ratio at time indicated

whole rock samples has not been changed (via thermal events, fluid flow) between the time of comparison at 1,736 Ma and the present day.

For the model invoking remobilization of syngenetic ore, whereby the origin of Homestake epigenetic gold mineralization is attributed to dissolution, mobilization, and re-concentration of older exhalative ore during regional metamorphism, evidence of the crustal prehistory should be evident in the sulfide Os_i ratio. The determined Os_i ratio for Homestake arsenopyrite is quite unradiogenic (0.28 ± 0.15), however, meaning extensive input of Os from older ore is unlikely and thus does not support this model. Although difficult to precisely quantify, transfer of this Os isotopic signature to Homestake sulfides by a remobilizing fluid would only be feasible if the original syngenetic ore had a near chondritic Os_i and a very low Re content (i.e., a $^{187}\text{Re}/^{188}\text{Os} < 50$); such Re–Os isotopic compositions are inconsistent with the observed compositions for Homestake iron formation, especially considering that Rye et al. (1974) proposed an age of 2.5 Ga for the iron formation (i.e., the presumed gold source) based on the measured Pb isotopic compositions of Homestake galena.

The metamorphic dehydration model is also difficult to reconcile with the representative whole rock compositions, all of which are characterized by $^{187}\text{Os}/^{188}\text{Os}$ ratios at 1,736 Ma that are far too radiogenic to have feasibly contributed Os to the ore-forming system. This inference is consistent with modeling of the Os isotopic evolution of continental crust (Fig. 10), which also yields $^{187}\text{Os}/^{188}\text{Os}$ ratios more radiogenic than that of Homestake arsenopyrite at 1,736 Ma. One specific suggestion, forwarded by Caddey et al. (1991) on the basis of work on Archean greenstone-hosted gold by Groves et al. (1987), is that mafic–ultramafic rocks in Precambrian greenstone belts could ultimately represent the source of gold in orogenic deposits, such as Homestake. The most voluminous sequence of mafic rocks known in the northern Black Hills is the Yates member of the Poorman Formation which comprises tholeiitic meta-basalts that were deposited in a backarc basin setting (Redden et al. 1990; Caddey et al. 1991), perhaps at 2,012 Ma (Hark et al. 2008). The single analyzed sample of Yates amphibolite is characterized by a radiogenic $^{187}\text{Os}/^{188}\text{Os}$ ratio of ~ 1.9 at 1,736 Ma. The relatively rapid Os isotopic evolution of this basalt is produced by its elevated $^{187}\text{Re}/^{188}\text{Os}$ ratio ($=269$; Table 4), consistent with that of mid-ocean ridge basalts in general (100–5,000; Shirey and Walker 1998). If this indeed reflects the original Os isotopic compositions of the amphibolite, it results in the generation of $^{187}\text{Os}/^{188}\text{Os}$ ratios at 1,736 Ma that are too radiogenic to have provided the source of Os to the arsenopyrite.

Models invoking derivation of Homestake ore fluids/metals directly from granitic magmas at ca. 1,730 Ma suffer

from the same problems as the remobilized syngenetic and metamorphic dehydration models in that these peraluminous magmas are derived from partial melting of Archean and Paleoproterozoic metasedimentary rocks (Nabelek and Bartlett 1998; Nabelek and Liu 1999) with $^{187}\text{Os}/^{188}\text{Os}$ ratios at 1,730 Ma that were too radiogenic in comparison to that of the arsenopyrite. In the absence of a more suitable explanation, the initial Os isotopic composition of Homestake arsenopyrite might best be attributed to the presence in the hydrothermal system of osmium derived from deep-seated, juvenile melts emplaced at ca. 1,730 Ma, from older, Re-depleted juvenile melts, or possibly even directly from the mantle. Considering the lack of exposed mafic rocks of suitable character in the northern Black Hills, a possible scenario is one in which the mantle supplied a component of heat to the deep crust, possibly in the form of underplating mafic melts not exposed at present erosional levels that resulted in peak metamorphism at ca. 1,750 Ma and/or generation of crustal melts starting at ca. 1,730 Ma. This input of mantle-derived material would also have contributed some fluids and metals to the Homestake mineralizing system, possibly including gold. This interpretation is consistent with existing models that invoke thinning of the subcrustal lithosphere and an increase in mantle heat flux as the trigger for Harney Peak granite magmatism (Holm et al. 1997; Holm 1999), but is at variance with models that view generation of the granite magmatism as a result of shear heating induced by Wyoming-Superior continental collision (Nabelek and Liu 1999).

Assessment of apparent Re–Os chronometer closure temperatures

The closure temperature of a mineral chronometer is “the temperature of the system at the time represented by its apparent age” (Dodson 1973). In other words, the closure temperature of a particular geochronometer reflects its ability to “see through” geologic events by retention of primary age information. The new and existing age constraints for Homestake gold mineralization, coupled with knowledge of the syn- and post-mineralization thermal history of the region, allow for estimations of apparent closure temperatures of the Re–Os arsenopyrite and pyrrhotite chronometers.

The preservation of a Re–Os isochron by arsenopyrite that yields a result within the existing age window for gold mineralization at Homestake suggests that no isotopic disturbance of Re and Os has occurred since its crystallization. Peak regional metamorphism in the Black Hills was contemporaneous with D_2 deformation during continental collision between the Wyoming and Superior cratons (Dahl et al. 1999). This prolonged metamorphic event was

initiated throughout the Black Hills at ca. 1,760–1,750 Ma (Dahl and Frei 1998; Dahl et al. 2005a, b) and resulted in prograde garnet growth in the Homestake area by ca. 1,745 Ma, prior to main-stage gold mineralization (Frei et al. 2009). Peak metamorphic pressure and temperature in the Homestake area are constrained by the position of the biotite–garnet isograd within the deposit and have been estimated by Kath and Redden (1990) at 2 to 4.5 kbar and 500°C, respectively. This peak temperature estimate coincides with that previously determined by Chinn (1969) (500±50°C) from Fe–Mg compositions of coexisting biotite and garnet in the Homestake host rocks, but is slightly lower than that suggested by Caddey et al. (1991) (540°C). Prevailing ambient temperatures during subsequent retrograde metamorphism and hydrothermal activity in the Homestake area at the time of gold mineralization (ca. 1,730 Ma, this study) are less constrained, but available data from arsenopyrite geothermometry (465–535°C; Sharp et al. 1985) indicate that an elevated temperature regime was maintained. This temperature regime possibly coincides with the early stages of granite magmatism in the northern Black Hills and continued until the end of magmatism at ca. 1,690 Ma (Fig. 8). Elevated temperature conditions prevailed until 1,500–1,300 Ma, at which time regional temperatures finally cooled below the closure temperatures of the $^{40}\text{Ar}/^{39}\text{Ar}$ muscovite (~350°C) and biotite (~300°C) chronometers (Holm et al. 1997; Dahl et al. 1999; Dahl and Foland 2008). Based on the determined Re–Os ages and on these existing temperature constraints, the minimum apparent closure temperature for the Re–Os arsenopyrite chronometer is conservatively estimated at 400°C and probably exceeds 450°C.

In contrast to arsenopyrite, the highly scattered Re–Os pyrrhotite analyses yield a highly imprecise age result (1,558±680 Ma) that, in this instance, shows pyrrhotite to be unreliable for dating ore mineralization. Given that the pyrrhotite analyses contained negligible blank contributions and that sufficiently high amounts of radiogenic Os ($^{187}\text{Os}^*$) were analyzed (1.2–4.2 pg) to yield precision of better than 0.2% SE on raw measured $^{187}\text{Os}/^{188}\text{Os}$ ratios, analytical effects can effectively be ruled out as the source of the observed scatter. An alternative possibility is the occurrence of the Claus process upon sample digestion, whereby Fe in the sample promotes oxidation of H_2S to elemental S and consequently inhibits the oxidation of Os required for sample spike equilibration (Frei et al. 1998). However, if it occurred during digestion, this reaction did not affect Os isotopic compositions of Homestake pyrrhotite because in contrast to the findings of Frei et al. (1998), no decrease in Os yield was observed between analyses of higher (>400 mg) vs. lower (<250 mg) sample weights. Moreover, even analyses of low sample weights (e.g., P1d, P2d; Table 2), in which the effects of the Claus process

should be minimized, yielded scattered results (Fig. 6b). The simplest interpretation of this result is that the Re–Os system in Homestake pyrrhotite has been disturbed subsequent to its primary crystallization. This interpretation is consistent with experimental results that show measurable diffusion of Os in pyrrhotite at temperatures as low as 400°C and on timescales <500,000 years (Brenan et al. 2000). In a study of Voisey’s Bay magmatic nickel sulfide system, Lambert et al. (2000) provide further support for open-system behavior of this mineral with respect to Re–Os. Regression of a six-point multi-mineral isochron from the Voisey’s Bay intrusion, including one pyrrhotite point, defines an age ~300 million years younger than the true mineralization age, a result attributed to mineral-scale disturbance during a Grenvillian (1.0 Ga) hydrothermal overprint. Frei et al. (1998) also question the ability of pyrrhotite to retain primary Re–Os data in their study of shear zone-hosted gold deposits in the Harare-Shamva Greenstone Belt, Zimbabwe. Two Re–Os analyses of pyrrhotite from the Kimberley mine plot well below a 1,960 Ma Re–Os reference isochron defined by analyses of molybdenite-bearing scheelite and are interpreted to reflect disturbance during post-crystallization, low-temperature alteration.

Considering the above arguments, the 1,558±680 Ma result for Homestake pyrrhotite is interpreted to confirm open system Re–Os systematics during prolonged slow cooling in the Black Hills until ca. 1,300 Ma. Consistent with the experimental results of Brenan et al. (2000), the closure temperature of pyrrhotite is constrained to be <400°C and is most likely ~300–350°C, in a range similar to the closure temperatures of the $^{40}\text{Ar}/^{39}\text{Ar}$ biotite and muscovite chronometers.

Conclusions

Re–Os geochronology of arsenopyrite from the Homestake gold deposit indicates that the emplacement of cogenetic gold occurred at 1,736±8 Ma, during or shortly after attainment of peak metamorphic conditions. This result agrees with previously established age brackets for the timing of gold mineralization, further validating arsenopyrite as a reliable chronometer for dating hydrothermal ore formation. Based on this new result and existing geochronology for rocks of the Black Hills, this large gold mineralizing event is proposed to have occurred at 1,730 Ma, almost simultaneously with both the onset of differential uplift and exhumation of crustal blocks and, possibly, the earliest intrusive phases of Harney Peak granite magmatism. New U–Pb data from in situ thin section monazite spot analyses by laser ablation ICP-MS confirm that the Harney Peak magmatic event(s) was

protracted, lasting until at least about 1,690 Ma. Initial $^{187}\text{Os}/^{188}\text{Os}$ ratios derived from the arsenopyrite isochron regression are unradiogenic, indicating input of Os from mantle, very juvenile crust, or older Re-depleted rocks into the Homestake mineralizing system.

In contrast to arsenopyrite, Re–Os isotopic analyses of Homestake pyrrhotite yield highly scattered results and an anomalously young, highly imprecise “age” of $1,558 \pm 680$ Ma. This result is interpreted to reflect post-crystallization isotopic disturbance during prolonged, post-orogenic cooling of rocks in the Black Hills. Together with proposed temperature estimates for rocks of the northern Black Hills during and following peak metamorphism, the Re–Os arsenopyrite age is suggestive of a *minimum* closure temperature for this chronometer in the 400–500°C range. In contrast, the Re–Os pyrrhotite result confirms a *maximum* closure temperature for this chronometer that is similar to that of the of $^{40}\text{Ar}/^{39}\text{Ar}$ biotite and muscovite chronometers (i.e., 300–350°C).

Acknowledgments Funding for this research was provided by an Alberta Ingenuity Studentship and a Society of Economic Geologists student research grant to RMM, and an NSERC Discovery Grant to RAC. Gayle Hatchard, Jaime Donnelly, GuangCheng Chen, Sergei Matveev, Rajeev Nair, and Diane Caird are gratefully acknowledged for technical support at the University of Alberta. We acknowledge the logistical support of the staff at the Homestake Mine; mine geologists James Berry, David Thornton, Tom Transinger and, in particular, chief geologist Bruce McDonald for granting access to the mine. We would like to thank Barrick Gold Corporation staff John McDonough and Karl Burke for coordinating and supplying data and Laurie Gehner for assistance with drill, assay, and section data. CCB would like to thank Mike Terry for his wealth of knowledge on the Homestake Mine and Black Hills and for logistical support and Colin Paterson for access to his photographic library and for use of facilities at the South Dakota School of Mines and Technology. CCB gratefully acknowledges the Departamento de Geodinamica at the Universidad de Granada where part of the research for this paper was undertaken and the facilities provided by the School of Earth Science at James Cook University. The Radiogenic Isotope Facility at the University of Alberta is supported, in part, by an NSERC Major Resources Support Grant. Fernando Barra and an anonymous reviewer are thanked for insightful reviews of the manuscript.

References

- Arne DC, Bierlein FP, Morgan JW, Stein HJ (2001) Re–Os dating of sulfides associated with gold mineralization in central Victoria, Australia. *Econ Geol* 96:1455–1459
- Bachman RL, Sneyd DS, Campbell TJ (1990) The Crook Mountain Granite and its possible relation to Early Proterozoic gold mineralization, Homestake Mine, Black Hills, South Dakota. *Abstr Programs Geol Soc Amer, Rocky Mountain Section* 22:A2
- Birck JL, RoyBarman M, Capmas F (1997) Re–Os measurements at the femtomole level in natural samples. *Geostand News* 20:19–27
- Brenan JM, Cherniak DJ, Rose LA (2000) Diffusion of osmium in pyrrhotite and pyrite: implications for closure of the Re–Os isotopic system. *Earth Planet Sci Lett* 180:399–413
- Caddey SW, Bachman RL, Campbell TJ, Reid RR, and Otto RP (1991) The Homestake gold mine, an early Proterozoic iron-formation-hosted gold deposit, Lawrence County, South Dakota. *United States Geological Survey Bulletin* 1857-J, 67 pp
- Chinn W (1969) Structural and mineralogical studies at the Homestake Mine, Lead, South Dakota. PhD dissertation, University of California, Berkeley, California
- Cohen AS, Waters FG (1996) Separation of osmium from geological materials by solvent extraction for analysis by TIMS. *Analytical Chimica Acta* 332:269–275
- Connolly JP (1927) The Tertiary mineralization of the northern Black Hills. *South Dakota School of Mines and Technology Bulletin* 15, 130 pp
- Creaser RA, Papanastassiou DA, Wasserburg GJ (1991) Negative thermal ion mass spectrometry of osmium, rhenium, and iridium. *Geochim Cosmochim Acta* 55:397–401
- Dahl PS, Foland KA (2008) Concentric slow cooling of a low-P–high-T terrane: evidence from 1600–1300 Ma mica dates in the 1780–1700 Ma Black Hills Orogen, South Dakota, U.S.A. *Am Mineral* 93:1215–1229
- Dahl PS, Frei R (1998) Step-leach Pb–Pb dating of inclusion-bearing garnet and staurolite, with implications for Early Proterozoic tectonism in the Black Hills collisional orogen, South Dakota, United States. *Geology* 26:111–114
- Dahl PS, Holm DK, Gardner ET, Hubacher FA, Foland KA (1999) New constraints on the timing of Early Proterozoic tectonism in the Black Hills (South Dakota), with implications for docking of the Wyoming province with Laurentia. *Geol Soc Amer Bull* 111:1335–1349
- Dahl PS, Hamilton MA, Jercinovic MJ, Terry MP, Williams ML, Frei R (2005a) Comparative isotopic and chemical geochronometry of monazite, with implications for the U–Th–Pb dating by electron microprobe: an example from the metamorphic rocks of the eastern Wyoming Craton (U.S.A.). *Am Mineral* 90:619–638
- Dahl PS, Terry MP, Jercinovic MJ, Williams ML, Hamilton MA, Foland KA, Clement SM, Friberg LM (2005b) Electron probe (Ultrachron) microchronometry of metamorphic monazite: unraveling the timing of polyphase tectonism in the easternmost Wyoming Craton (Black Hills, South Dakota). *Am Mineral* 90:1712–1728
- Dahl PS, Hamilton MA, Wooden JL, Foland KA, Frei R, McCombs JA, Holm DK (2006) 2480 Ma mafic magmatism in the northern Black Hills, South Dakota: a new link connecting the Wyoming and Superior cratons. *Can J Earth Sci* 43:1579–1600
- DeWitt ED, Redden JA, Busher D, Wilson AB (1989) Geologic map of the Black Hills area, South Dakota and Wyoming. *US Geological Survey Miscellaneous Investigations Series Map I-1910*, scale 1:250,000
- Dodson MH (1973) Closure Temperature in Cooling Geochronological and Petrological Systems. *Contrib Mineral Petrol* 40:259–274
- Frei R, Nägler Th F, Schönberg R, Kramers JD (1998) Re–Os, Sm–Nd, U–Pb, and stepwise leaching isotope systematics in shear-zone hosted gold mineralization: genetic tracing and age constraints of crustal hydrothermal activity. *Geochim Cosmochim Acta* 62:1925–1936
- Frei R, Dahl PS, Frandsson MM, Jensen LA, Hansen TR, Terry MP, Frei KM (2009) Lead-isotope and trace-element geochemistry of Paleoproterozoic metasedimentary rocks in the Lead and Rochford basins (Black Hills, South Dakota, USA): implications for genetic models, mineralization ages, and sources of leads in the Homestake gold deposit. *Precambrian Res* 172:1–24
- Ghosh A, Frei R, Whitehouse MJ, Dahl PS (2008) U–Pb geochronologic study of magmatic zircon in Paleoproterozoic granitic pegmatite and associated metapelites, Black Hills, South Dakota: implications for gold petrogenesis and sedimentary Provenance. *Geological Society of America Abstracts with Programs* 40(6):145

- Goldfarb RJ, Groves DI, Gardoll S (2001) Orogenic gold and geologic time: a global synthesis. *Ore Geol Rev* 18:1–75
- Goldfarb RJ, Baker T, Dubé B, Groves DI, Hart CJR, Gosselin P (2005) Distribution, character, and genesis of gold deposits in metamorphic terranes. In: Hedenquist JW, Thompson JFH, Goldfarb RJ, Richards JP (eds) *Econ Geol 100th Anniversary Volume*, Soc Econ Geol, pp 407–451
- Groves DI, Phillips GN, Ho SE, Houston SM, Standing CA (1987) Craton-scale distribution of Archean greenstone gold deposits; predictive capacity of the metamorphic model. *Econ Geol* 82:2045–2058
- Groves DI, Goldfarb RJ, Gebre-Mariam M, Hagemann SG, Robert F (1998) Orogenic gold deposits: a proposed classification in the context of their crustal distribution and relationship to other gold deposit types. *Ore Geol Rev* 13:7–27
- Gustafson JK (1933) Metamorphism and hydrothermal alteration of the Homestake gold-bearing formation. *Econ Geol* 28:123–262
- Hark JS, Frei R, Whitehouse MJ, Dahl PS (2008) New evidence for 2.01 Ga rifting of the easternmost Wyoming craton (Black Hills, SD): implications for break-up of a supercraton (Superia). *Geological Society of America Abstracts with Programs* 40 (6):145
- Holm DK (1999) A geodynamic model for Paleoproterozoic post-tectonic magma genesis in the southern Trans-Hudson (Black Hills, South Dakota) and Penokean (southern Lake Superior) orogens. *Rocky Mountain Geology* 34:183–194
- Holm DK, Dahl PS, Lux DR (1997) $^{40}\text{Ar}/^{39}\text{Ar}$ evidence for Middle Proterozoic (1300–1500 Ma) slow cooling of the southern Black Hills, South Dakota, midcontinent, North America: implications for Early Proterozoic P–T evolution and posttectonic magmatism. *Tectonics* 16:609–622
- Hosted JO, Wright LB (1923) Geology of the Homestake ore bodies and the Lead area of South Dakota. *Eng Min J Press* 115:793–799
- Houston RS (1992) Proterozoic mineral deposits near plate margins of the Archean Wyoming Province, USA. *Precambrian Res* 58:85–97
- Kath RL (1990) Petrogenesis of the Homestake iron formation and associated pelitic rocks, Lead, South Dakota: Implications for P–T paths, fluid evolution, and gold mineralization. Unpublished Ph.D. dissertation, South Dakota School of Mines and Technology, 228p
- Kath RL, Redden JA (1990) Petrogenesis of the Homestake iron formation, Lead, South Dakota; assemblages of metamorphism. In: Paterson CJ, Lisenbee AL (eds) *Metallogeny of gold in the Black Hills, South Dakota*. Society of Economic Geologists Guidebook Series Volume 7:112–118
- Krogstad EJ, Walker R (1994) High closure temperatures of the U–Pb system in large apatites from the Tin Mountain Pegmatite, Black Hills, South Dakota, USA. *Geochimica et Cosmochimica Acta* 58:3845–3853
- Lambert DD, Frick LR, Foster JG, Li C, Naldrett AJ (2000) Re–Os isotope systematics of the Voisey's Bay Ni–Cu–Co magmatic sulfide system, Labrador, Canada: II. Implications for parental magma chemistry, ore genesis, and metal redistribution. *Econ Geol* 95:867–888
- Ludwig KR (2003) Isoplot 3.00, a geochronological toolkit for Microsoft Excel: Berkeley Geochronology Center Special Publication No. 4
- Mathur R, Ruiz J, Munizaga F (2000) Relationship between copper tonnage of Chilean base-metal porphyry deposits and Os isotope ratios. *Geology* 28:555–558
- Meier LF (1992) Structure and ore trend description of the Homestake Mine. In: Paterson CJ, Lisenbee AJ (eds) *Metallogeny of gold in the Black Hills, South Dakota*. Society of Economic Geologists Guidebook Series, Volume 7
- Meisel T, Walker RJ, Irving AJ, Lorand J (2001) Osmium isotopic compositions of mantle xenoliths: a global perspective. *Geochim Cosmochim Acta* 65:1311–1323
- Morelli RM, Creaser RA, Selby D, Kelley KD, Leach DL, King AR (2004) Re–Os sulfide geochronology of the red dog sediment-hosted Zn–Pb–Ag deposit, Brooks Range, Alaska. *Econ Geol* 99:1569–1576
- Morelli RM, Creaser RA, Selby D, Kontak DJ, Horne RJ (2005) Rhenium–osmium geochronology of arsenopyrite in Meguma Group gold deposits, Meguma Terrane, Nova Scotia, Canada: evidence for multiple gold-mineralizing events. *Econ Geol* 100:1229–1242
- Morelli RM, Creaser RA, Seltmann R, Stuart FM, Selby D, Graupner T (2007) Age and source constraints for the giant Muruntau gold deposit, Uzbekistan, from coupled Re–Os–He isotopes in arsenopyrite. *Geology* 35:795–798
- Morgan JW, Golightly DW, Dorrzapf AF (1991) Methods for the separation of rhenium, osmium and molybdenum applicable to isotope geochemistry. *Talanta* 38:259–265
- Nabelek PI, Bartlett CD (1998) Petrologic and geochemical links between the post-collisional Proterozoic Harney Peak leucogranite, South Dakota, U.S.A., and its source rocks. *Lithos* 45:71–85
- Nabelek PI, Liu M (1999) Leucogranites in the Black Hills of South Dakota: the consequence of shear heating during continental collision. *Geology* 27:523–526
- Noble JA (1950) Ore mineralization in the Homestake gold mine. *Geol Soc Amer Bull* 61:221–252
- Paige S (1924) Geology of the region around lead, South Dakota. *US Geological Survey Bulletin* 765:56
- Paterson CJ, Lisenbee AL (1990) Introduction. In: Paterson CJ, Lisenbee AL (eds) *Metallogeny of gold in the Black Hills, South Dakota*. Society of Economic Geologists Guidebook Series Volume 7:103–111
- Peucker-Ehrenbrink B, Jahn B (2001) Rhenium–osmium isotope systematics and platinum group element concentrations: loess and the upper continental crust. *Geochem Geophys Geosyst* 2:1061. doi:10.1029/2001GC000172
- Redden JA, French G (1989) Geologic setting and potential exploration guides for gold deposits, Black Hills, South Dakota. *US Geological Survey Bulletin* 1857-B:B45–B72
- Redden JA, Peterman ZE, Zartman RE, DeWitt E (1990) U–Th–Pb zircon and monazite ages and preliminary interpretation of the tectonic development of Precambrian rocks in the Black Hills. In: Lewry JF, Stauffer MR (eds) *The early proterozoic Trans-Hudson Orogen of North America*. Geological Association of Canada Special Paper 37, pp 229–251
- Reid RR (1982) Structural geology of the Homestake Mine, Lead, South Dakota: internal summary report. Homestake Mine, South Dakota
- Rye DM, Rye RO (1974) Homestake gold mine, South Dakota: I. Stable isotope studies. *Econ Geol* 69:293–317
- Rye DM, Doe BR, Delevaux MH (1974) Homestake gold mine, South Dakota: II. Lead isotopes, mineralization ages, and source of lead in ores of the northern Black Hills. *Econ Geol* 69:814–822
- Schmitz MD, Schoene B (2006) Derivation of isotope ratios, errors, and error correlations for U–Pb geochronology using ^{205}Pb – ^{235}U –(^{233}U)-spiked isotope dilution thermal ionization mass spectrometric data. *Geochem Geophys Geosyst* 8:Q08006. doi:10.1029/2006GC001492
- Selby D, Creaser RA (2001a) Late and Mid-Cretaceous mineralization in the northern Canadian Cordillera: constraints from Re–Os molybdenite dates. *Econ Geol* 96:1461–1467
- Selby D, Creaser RA (2001b) Re–Os geochronology and systematics in molybdenite from the Endako porphyry molybdenum deposit, British Columbia, Canada. *Econ Geol* 96:197–204

- Sharp ZD, Essene EJ, Kelly WC (1985) A re-examination of the arsenopyrite geothermometer; pressure considerations and applications to natural assemblages. *Can Mineral* 23:517–534
- Shirey SB, Walker RJ (1995) Carius tube digestion for low-blank rhenium-osmium analysis. *Anal Chem* 67:2136–2141
- Shirey SB, Walker RJ (1998) The Re–Os isotope system in cosmochemistry and high-temperature geochemistry. *Ann Rev Earth Planet Sci* 26:423–500
- Simonetti A, Heaman LM, Chacko T, Banerjee NR (2006) In situ petrographic thin section U–Pb dating of zircon, monazite, and titanite using laser ablation-MC-ICP-MS. *Int J Mass Spectrom* 253:87–97
- Sirbescu M-LC, Nabelek PI (2003) Crystallization conditions and evolution of magmatic fluids in the Harney Peak Granite and associated pegmatites, Black Hills, South Dakota—evidence from fluid inclusions. *Geochim Cosmochim Acta* 67:2443–2465
- Slaughter AL (1968) The Homestake Mine. In: Ridge JD (ed) *Ore deposits of the United States, 1933–1967 (vol II)*. American Institute of Mining and Metallurgy, Petroleum Engineers, New York, pp 1436–1459
- Smoliar MI, Walker RJ, Morgan JW (1996) Re–Os ages of Group IIA, IIIA, IVA and IVB iron meteorites. *Science* 271:1099–1102
- Stein HJ, Morgan JW, Scherstén A (2000) Re–Os dating of low-level highly radiogenic (LLHR) sulfides: the Harnäs gold deposit, southwest Sweden, records continental-scale tectonic events. *Econ Geol* 95:1657–1671
- Stein HJ, Markey RJ, Morgan JW, Hannah JL, Schertén A (2001) The remarkable Re–Os chronometer in molybdenite: how and why it works. *Terra Nova* 13:479–486
- Sun W, Bennett VC, Eggins SM, Kamenetsky VS, Arculus RJ (2003) Enhanced mantle-to-crust rhenium transfer in undegassed arc magmas. *Nature* 22:294–297
- Terry MP, Dahl PS, Frei R (2003) Isotopic and geothermometric constraints on the structural evolution of Homestake gold deposit, Black Hills, South Dakota (USA). *European Geophysical Society, Geophysical Research Abstracts* 5:13191
- Völkening J, Walczyk T, Heumann K (1991) Osmium isotopic ratio determinations by negative thermal ionization mass spectrometry. *Int J Mass Spectrom Ion Phys* 105:147–159
- Williams ML, Jercinovic MJ, Hetherington CJ (2007) Microprobe monazite geochronology: understanding geologic processes by integrating composition and chronology. *Ann Rev Earth Planet Sci* 35:137–175